



Batch ED fed by a PV unit: a reliable, flexible, and sustainable integration

F. Círez^a, J. Uche^{a,*}, A.A. Bayod^b, A. Martínez^a

^a*Circe Foundation, University of Zaragoza, Mariano Esquillor 15, 50018, Zaragoza, Spain
Tel. +34 976 76 25 84; Fax: +34 976 73 20 78; email: javiuche@unizar.es*

^b*Department of Electrical Engineering, University of Zaragoza, Zaragoza, Spain*

Received 29 February 2012; Accepted 15 June 2012

ABSTRACT

Electrodialysis (ED) is a reliable technique to produce drinking water from brackish raw water sources. If the ED unit is fed by a photovoltaic (PV) generator, water production maybe also understood as sustainable. In this paper, the feasibility of a small and easily operating batch ED pilot plant powered by PV modules or by a rectifier (electrical grid connection) was studied in depth. First, a mathematical model was implemented in order to predict the batch ED-FV pilot plant behavior. Then, numerous tests were carried out at the experimental installation. Some relevant parameters were studied: the influence of NaCl concentration (600–10,000 ppm), the applied voltage (8–12 V), and the configuration of PV array, as well as environmental conditions. Different optimal operating conditions were investigated depending on the batch ED energy source: if the ED stack was fed by the rectifier, the lowest specific energy consumption or maximal production was followed. On the contrary, when it was fed by the PV array, the maximum power production of the PV modules was pursued. This maximum PV power depended on irradiation, ambient temperature, and solutions concentration, and consequently varied along any test.

Keywords: Brackish desalination; Electrodialysis; Photovoltaics; Modeling; ED-PV pilot plant

1. Introduction

During the twentieth century, the growth in world population and industrial development provoked a continuous rise in water consumption. It is quite common to find out an unbalanced situation between the number of inhabitants and the carrying capacity of local renewable water resources. Thus, development of reliable, relatively simple, and new drinking water systems becomes indispensable in water stressed regions [1]. Fortunately, most of those water scarce

areas present two interesting features: large brackish underground resources and high average annual irradiation. This implies that solar energy could be considered as the unique energy source for brackish water desalination in those regions.

The use of solar energy to fed desalination technologies has been well reported. For instance distillation technologies like multieffect distillation or membrane distillation, [2–5] have been coupled with diverse solar thermal technologies, and power consumed by reverse osmosis (RO) could be produced by thermal sources [6] or photovoltaics (PV) modules [7,8]. However, the combination of electrodialysis (ED) and PV for

*Corresponding author.

brackish water desalination is still being developed and not much literature has been published yet. Anyway, some theoretical and experimental studies [9,10] have shown that ED-PV systems present very promising results for desalting brackish water (in terms of low specific energy consumption (SEC)), being the ED powered by batteries or directly by PV modules.

ED is an electrochemical process aimed to the separation of ions across charged membranes from one solution to another, under the influence of an electrical potential difference. In a typical ED cell, a series of anion and cation exchange membranes (AIM and CIM, respectively) are arranged in an alternating pattern between an anode and a cathode to form individual cells. When a direct current (DC) potential is applied between two electrodes, the positively charged ions move to the cathode, passing through the negatively charged CIM and being retained by the positively charged AIM. On the other hand, the negatively charged ions move to the anode, pass through the AIM and are stopped by the CIM. At the end, ion concentrations increase in alternating compartments, with a simultaneous decrease in ions in other compartments [11]. ED is competitive with respect to RO in low salty brackish desalination, especially in reused waters because of its lower sensibility to biological pollution. As the process requires the input of a DC power, PV systems become attractive for areas with abundant solar energy availability through the year. Moreover, PV systems usually require low maintenance costs [12].

In this paper, the mathematical model of a small batch ED stack unit powered by electrical power system by using a rectifier alternating current (AC)-DC converter system or powered directly by PV has been developed. The model was validated by a set of experimental tests developed at the batch ED-PV pilot plant. Tests were also performed to search the best operating conditions to the ED stack: minimum

energy consumption (grid connected to ED) or maximum power generation by the PV array.

2. Experimental facilities

The experimental setup is shown in Fig. 1. It comprises an ED pilot plant (EUR 2B-10P) manufactured by EURODIA, which is coupled to 1–4 PV modules.

2.1. Electrodialysis plant

The electric stage of this plant consists of a membrane stack with 10 ionic cell pairs and an optional rectifier which converts 230 VAC into a 60 V/10 A DC. Each pair of cells is configured with an anionic AMX-Sb and a cationic CMX-Sb membrane. These membranes have 2 dm² of active area per cell and a total active surface of 0.2 m². The hydraulic stage of the plant consists of three 100 W pumps and four rotameters that impulse the electrolyte, dilute, and brine solutions operating in batch with recirculation feeding.

Electrolyte, dilute, and brine tanks have a volume of 2.5 L, and rotameters flow were set at 180 L/h for dilute and brine solutions and 400 L/h for electrolyte solution (200 L/h per electrode), according to manufacturer instructions [13].

2.2. Photovoltaic modules

The PV modules were designed and manufactured according to the ED stack physical characteristics. As the number of ionic membranes connected in serial is reduced, the voltage applied to the stack was the main variable when the PV system was designed. According to the manufacturer data sheet [13], total voltage and current should not reach to 14 V and 7.2 A, respectively. However, commercial PV modules are

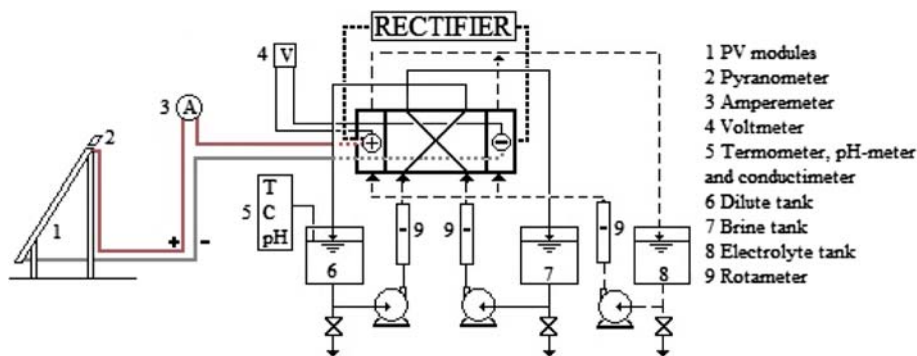


Fig. 1. Schema of ED-PV setup.

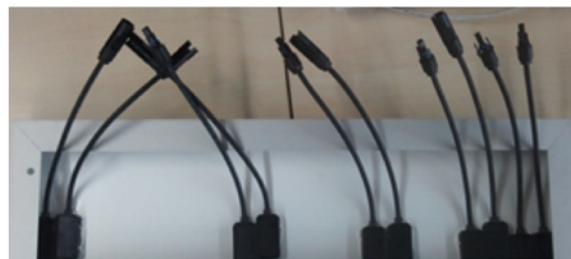
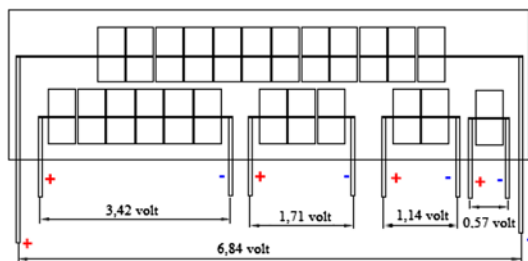


Fig. 2. Schema and picture of experimental PV modules.

designed to provide higher voltages, so there was a need to design specific PV modules which were able to provide a maximum open-circuit voltage of 14 V. Four experimental PV modules were specifically developed in collaboration to a Spanish PV manufacturer. Definite PV arrangement consisted of 24 solar cells (one-sixth of a Quantum Solar polycrystalline wafer) and was encapsulated in the same way as commercial modules. Those modules have 10 connectors so that cells could be connected in serial one by one (from 1 to 24), thus providing a short-circuit current of 1 A and an open-circuit voltage from 0.57 V up to 13.7 V. A schema of front and a picture of back view of those modules are presented in Fig. 2.

2.3. Instrumentation

As shown in Fig. 1, four *in situ* measurement instruments were installed at the experimental setup. Number two makes reference to a Mcsolar (SolarC) equivalent technology cell irradiation meter; numbers three and four are an amperemeter and voltmeter, respectively; and number five is a conductivity/pH/temperature lecturer (MM40+ with a 5059P Crisom probe).

In order to check the validity of the model (only sodium and chloride ions were considered in mathematical model), NaCl with 99.9% of purity and distillate water (10 μ S/cm of conductivity) were mixed to produce from 600 up to 10,000 ppm NaCl solutions. As electrolyte, and according to ED manufacturer guidelines [13], a 20 mS/cm solution of Na₂SO₄ (99% of purity) was used.

3. Theoretical model

The usefulness of a mathematical simulation model resides on the prediction the ED-PV performance upon diverse operating conditions, as well as to search for the best configuration that match, as better as possible, the ED stack and PV field, taking into account that the ED load (electrical resistance of brackish water) increases as water is becoming free of

salts. The model was based on the application of mass transport equations on the ED stack and the set of equations corresponding to the equivalent electrical circuit of a PV system. As model inputs, feedwater concentration, applied voltage, irradiation, ambient temperature, and PV configuration were considered. Batch time could be also imposed to the model, if desired.

3.1. Modeling the PV generator

There are several mathematical models in the literature to describe PV generators, from simple to more complex ones. To simplify the parameter adjustment of the model, the one-diode model was used in which, according to the Shockley theory [14], recombination in the space charge zone is neglected.

A four elements model with a single diode was then considered here as the equivalent PV cell. The parameters of the equivalent five-parameter electrical circuit were extracted by solving a system of equations, which are based on the data-set provided by PV manufacturers in standard test conditions (STC) [15]. The basic model for a PV module is shown in Fig. 3, as well as the current–voltage (I–V) characteristic curve of a PV module which could be described with Eq. (1):

$$I = I_L - I_0 \left[\exp\left(\frac{V + IR_s}{mV_T}\right) - 1 \right] - \frac{V + IR_s}{R_{sh}} \quad (1)$$

where I_L is the light-generated current (A); I_0 is the reverse saturation current of the diode (A); R_s is the series resistance of the cells (Ohm); R_{sh} is the shunt resistance of the cells (Ohm); and m is a parameter that takes into account the ideality of the diode (*ideality factor*). V_T is the thermal voltage and depends on the cell temperature (V), which is defined as Eq. (2):

$$V_T = \frac{kT_c}{q} \quad (2)$$

where T_c is the cell temperature (K), k is the Boltzman constant (J K⁻¹), and q is the charge of the electron (C).

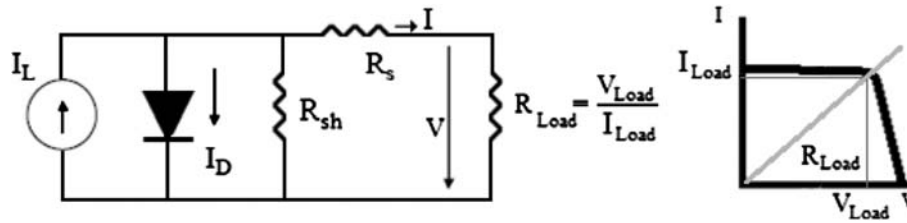


Fig. 3. Equivalent circuit in the four elements model (left) and I-V curve (right).

The four elements analytical model is an implicit nonlinear equation, which can be solved at any specific irradiation and cell temperature with numerical iterative techniques [15] since all the five parameters I_L , I_0 , R_s , R_{sh} , and m were previously given. Their relation with irradiation and cell temperature is shown in Eqs. (3)–(8).

$$I_L = I_{sc} \left(1 + \frac{R_s}{R_{sh}} \right) + I_0 \left[\exp \left(\frac{I_{sc} R_s}{m V_T} \right) - 1 \right] \quad (3)$$

where

$$I_0 = \left(I_{sc} - \frac{V_{oc}}{R_{sh}} \right) \exp \left(-\frac{V_{oc}}{m V_T} \right) \quad (4)$$

$$R_s = R_{so} - \left[\frac{m V_T}{I_0} \exp \left(-\frac{V_{oc}}{m V_T} \right) \right] \quad (5)$$

$$m = \frac{V_{mp} + I_{mp} R_{so} - V_{oc}}{V_T \left[\ln \left(I_{sc} - \frac{V_{mp}}{R_{sh}} - I_{mp} \right) - \ln \left(I_{sc} - \frac{V_{oc}}{R_{sh}} \right) + \left(\frac{I_{mp}}{I_{sc}} \frac{V_{oc}}{R_{sh}} \right) \right]} \quad (6)$$

$$I_{sc} = I_{sc,ref} \frac{G}{G_{ref}} + \alpha (T_c - T_{c,ref}) \quad (7)$$

and

$$V_{oc} = V_{oc,ref} + m V_T \ln \left(\frac{G}{G_{ref}} \right) + \beta (T_c - T_{c,ref}) \quad (8)$$

where I_{sc} (A) and V_{oc} (V) are the short-circuit current and open-circuit voltage, respectively; $I_{sc,ref}$ (A) and $V_{oc,ref}$ (V) are previous parameters at STC; I_{mp} (A) and V_{mp} (V) are the current and voltage at maximum power conditions; T_c is the cell temperature (K); $T_{c,ref}$ is the cell temperature at STC conditions (25°C); G is the irradiation (W/m^2); G_{ref} is the irradiation at STC conditions ($1,000 W/m^2$); α is the short-circuit current

variation coefficient with temperature ($A K^{-1}$); and β the open-circuit variation coefficient with temperature ($V K^{-1}$). All of these parameters are usually provided by the PV generator manufacturer. R_{so} is a theoretical parameter which could be estimated in 0.33 Ohm [16].

3.2. Modeling the ED stack

Mass balances in both reactor compartments (dilute and concentrate) and in the tanks were arranged in order to know the evolution of NaCl concentration for both solutions. To thereby determine the concentrations, the following assumptions were introduced in this batch process:

- Reactor's compartments were perfectly mixed.
- Volume of concentrate and dilute compartments were equivalent.
- Feeding flows were known and kept constant along the batch time period.
- Temperature of dilute and concentrate solutions remained constant at 25°C.

Consequently, and according to theoretical models [17–19], the mass balance equations are:

$$\begin{aligned} \frac{dC_{conc}}{dt} = & \frac{Q_{conc}(C_{conc}^{in} - C_{conc})}{NV_{comp}} + \frac{\phi I}{zFV_{comp}} \\ & - \frac{a_m D_a (C_{conc}^{AIM} - C_{dil}^{AIM})}{h_a V_{comp}} \\ & - \frac{a_m D_c (C_{conc}^{CIM} - C_{dil}^{CIM})}{h_c V_{comp}} \end{aligned} \quad (9)$$

$$\begin{aligned} \frac{dC_{dil}}{dt} = & \frac{Q_{dil}(C_{dil}^{in} - C_{dil})}{NV_{comp}} - \frac{\phi I}{zFV_{comp}} \\ & + \frac{a_m D_a (C_{conc}^{AIM} - C_{dil}^{AIM})}{h_a V_{comp}} \\ & + \frac{a_m D_c (C_{conc}^{CIM} - C_{dil}^{CIM})}{h_c V_{comp}} \end{aligned} \quad (10)$$

where Q_{conc} and Q_{dil} are the flow rates of concentrate and dilute solutions ($m^3 s^{-1}$); C_{k}^{in} and C_k are the concentrations of the dilute or concentrate solutions at the tank and at the outlet of the stack ($mol m^{-3}$); N is the number of cell pairs; V_{comp} is the volume of compartments between cells (m^3); φ is the current efficiency; I is the current flowing through the stack (A); z and F are the ion charge and Faraday constant ($C mol^{-1}$); a_m , h_a , and h_c are respectively the membrane effective area (m^2) and the anionic and the cationic membrane thickness (m); D_a and D_c are the diffusion coefficient of anion and cations across the membrane ($m^2 s^{-1}$); and C_{k}^{AIM} and C_{k}^{CIM} are the concentrations of concentrate or dilute solutions on the surface of the anionic and cationic membrane ($mol m^{-3}$).

Eqs. (9) and (10) show that concentration inside the reactor depends on the concentrations at the inlet of the electrolyzer, so it was also necessary to obtain the variation of the concentration and the volume of the solution inside the tanks. Eqs. (11)–(14) allowed calculation of those variations:

$$\frac{d(C_{conc}^{in} V_{conc}^T)}{dt} = Q_{conc}(C_{dil}^{in} - C_{dil}) + J_w a_m V_w (C_{dil}^{in} - C_{dil}) \quad (11)$$

$$\frac{d(C_{dil}^{in} V_{dil}^T)}{dt} = Q_{dil}(C_{dil}^{in} - C_{dil}) - J_w a_m V_w (C_{dil}^{in} - C_{dil}) \quad (12)$$

$$\frac{d(V_{conc}^T)}{dt} = \left(\frac{t_w I}{F a_m} + L_w (C_{conc}^{in} - C_{dil}^{in}) \right) N a_m V_w \approx 0 \quad (13)$$

$$\frac{d(V_{dil}^T)}{dt} = \left(\frac{t_w I}{F a_m} - L_w (C_{conc}^{in} - C_{dil}^{in}) \right) N a_m V_w \approx 0 \quad (14)$$

where V_{k}^T is the volume of the concentrate or dilute tank (m^3); J_w is the overall water transport through the electro-membranes from the dilute to concentrate stream because of the electro-osmosis process ($mol s^{-1} m^{-2}$); V_w is the molar volume of pure water ($m^3 mol^{-1}$); t_w is the water transport number; and L_w is the membrane constant for water transport by diffusion ($m s^{-1}$). During experimental tests, it was observed that the volume of water transferred from the dilute to concentrate tank was quantitatively insignificant. Thus, it could be assumed that dilute and concentrate volume tanks remained unchanged, and

therefore the second term at the right side of Eqs. (11) and (12) could be neglected, and Eqs. (13) and (14) were approximated to zero.

One additional equation was still required to solve the complete equations system. That last equation emerges from a potential drop really applied to the ED stack. The overall potential drop across an ED stack can be written as Eq. (15) [20]:

$$E - E_{el} + (E_j + E_D)N = I \cdot R = I(R_{conc} + R_{dil} + R_{MEM}) \quad (15)$$

where E_{el} is the electrode potential for the anode and cathode processes (V); R is the addition of the membranes resistance (R_{MEM}), the R_c and the R_{dil} (the bulk solutions conductivity resistance of the concentrate and dilute solution) (Ohm); and E_j and E_D are the overall junction and Donnan potential differences across the boundary layers and membranes of any cell, respectively (V).

Several studies [21,22] have determined that, when the ED stack is working at the ohmic region (see Fig. 4), the overall junction and Donnan potential can be neglected. Thus, as Eq. (16) indicates, the current that cross the stack depends on the total voltage applied to stack and their compartments, as well as the tanks concentration.

$$E = E_{el} + \frac{N \cdot I \cdot h}{a_{me}} \left(\frac{1}{\Lambda_{conc} C_{conc}} + \frac{1}{\Lambda_{dil} C_{dil}} \right) + N \cdot \frac{R_g T}{F} \times \ln \left(\frac{\chi_{conc}^{CIM} C_{conc}^{CIM} \chi_{conc}^{AIM} C_{conc}^{AIM}}{\chi_{dil}^{CIM} C_{dil}^{CIM} \chi_{dil}^{AIM} C_{dil}^{AIM}} \right) \quad (16)$$

In Eq. (16), h is the distance between membranes (m); Λ_k is the molar conductivity of dilute or concentrate solution ($S m^2 mol^{-1}$); which can be obtained with Falkenhagen equation (Eq. (17)); R_g is the gas-law universal constant ($J mol^{-1} K^{-1}$); T is the solution temperature (K); χ is the mean ionic coefficient ($S m^{-1}$)

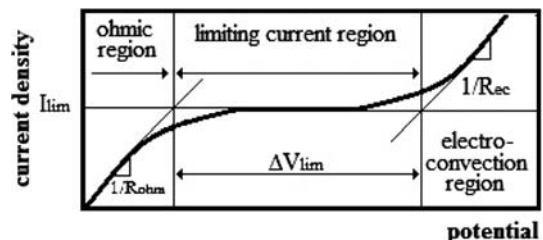


Fig. 4. Typical current–voltage curve for a cation exchange membrane showing the ohmic region, limiting current regions, and an overlimiting current [23].

Table 1
ED model parameters values

Parameter	Value	Source	Parameter	Value	Source
Q_{dil}, Q_{conc} ($m^3 s^{-1}$)	5×10^{-5}	[13]	h (m)	$6 \cdot 10^{-4}$	[26]
N	10	[13]	ρ_{AIM} (Ohm m^2)	18	[11]
V_{comp} (m^3)	6×10^{-6}	[26]	ρ_{CIM} (Ohm m^2)	12	[11]
ϕ	0.89	^a	E_{el} (V)	1.5	[26]
F (C mol^{-1})	96,485	–	R_g (J $mol^{-1} K^{-1}$)	8.31	–
a_m (m^2)	0.2	[13]	Λ_0 (S $m^2 mol^{-1}$)	1.162×10^{-3}	[28]
D_{ar}, D_c ($m^2 s^{-1}$)	3.28×10^{-11}	[27]	B_0 ($\text{Å}^{-1} mol^{-1/2}$)	3.277×10^{-1}	[28]
h_a (m)	1.4×10^{-4}	[13]	B_1 ($mol^{-1/2}$)	2.271×10^{-1}	[28]
h_c (m)	1.7×10^{-4}	[13]	B_2 (S $m^2 mol^{-3/2}$)	54.164	[28]
V_{concr}^T, V_{dil}^T (m^3)	2×10^{-3}	[13]	u (Å)	4	[28]

^aExperimentally obtained.

whose relation with concentration can be found in [24].

$$\Lambda = \Lambda_0 - (B_1 \Lambda_0 + B_2) \frac{\sqrt{C}}{1 + B_0 u \sqrt{C}} \quad (17)$$

In Eq. (17), Λ_0 , B_0 , B_1 , B_2 , and u are the Falkenhagen values for NaCl, which could be consulted at [25].

Once the ED and the PV subsystems were modeled, there were not significant differences between modeling an ED fed by rectifier or by the PV generators. In the first one (AC to DC current), the applied voltage was constant and known. So, current flowing through the stack could be obtained from Eq. (16). However, when the electrolyzer was fed by PV modules, the voltage was neither constant nor known, since it depended on the overall resistance at the ED stack and incoming irradiation and surrounding temperature. Anyway, the current and voltage from a PV generator provided at Eq. (1) and the modified Eq. (16) [25], allowed obtaining the slope of the line that

cross the I – V curve of the PV generator (Fig. 3), which finally provides the voltage and current applied to the ED stack (Eq. (18)):

$$\frac{E_{stack}}{I_{stack}} = R_{stack} \approx \frac{N}{a_m} \left(\frac{h}{\Lambda_{conc} C_{conc}} + \frac{h}{\Lambda_{dil} C_{dil}} + \rho_{CIM} h_c + \rho_{AIM} h_a \right) \quad (18)$$

In Eq. (18), ρ_{AIM} and ρ_{CIM} , are the anionic and cationic membrane resistances (Ohm m^2), whose values were obtained from bibliography [11]; and h_c and h_a are the cationic and anionic membrane thickness (m).

With these six Eqs. (1), (9)–(12), and (18), a Runge–Kutta method could be used to obtain a numerical solution providing the concentration and the current through the stack along the batch test.

Tables 1 and 2 show the values adopted for the parameters appearing from Eqs. (1)–(18), and their corresponding source.

Table 2
Parameters used to model the PV array

Parameter	Value	Source
k (J K^{-1})	$1.38 \cdot 10^{-23}$	–
q (C)	$1.6 \cdot 10^{-19}$	–
R_{sh} (ohm)	3,160	^a
$V_{oc,ref}$ (V/cell)	0.57	^a
$I_{sc,ref}$ (A)	1	^a
m	1.3	[29]
α (A K^{-1})	0.04	[29]
β (V K^{-1})	–0.021	[29]

^aExperimentally obtained.

4. Results and discussion

First, the comparison between mathematical model and the ED-FV pilot plant was studied. Then, the ED unit performance will be tested below diverse operating conditions: AC or DC (PV) power supply, raw water salinity, and environmental conditions.

4.1. Mathematical model validation

The results of the simulations are shown in the following. Fig. 5 illustrates the predicted and real variation of the dilute concentration inside the tank vs. the batch time for two different selected tests, both

starting from a raw water salinity of 5,000 ppm up to a product water of 250 ppm. One was fed by DC current (8V fixed) by means of the AC–DC rectifier; the other one used the PV modules.

The figure shows as the mathematical model successfully reproduced the experimental tests, providing no more than 5% of divergence between theoretical and experimental were found in all cases, being the highest gap in periods with large irradiation variability. Consequently, and taking into account this accuracy level, theoretical model could be considered as a predictive tool to anticipate the performance of the batch ED–PV pilot plant.

4.2. Optimal operating conditions, ED stack driven by rectifier

In order to obtain the influence of feedwater quality and voltage applied on SEC, raw solutions of various concentrations (580; 1,000; 2,000; 3,000; 5,000; 8,000; 9,000; and 10,000 ppm) were prepared and tested at 8, 10, and 12 V. In all cases, a product water of 250 ppm was intended at dilute tank. Fig. 6 shows as the SEC (kWh/m³) presents a linear behavior with

respect to the applied voltage (V) and feedwater concentration (ppm).

The energy analysis showed that the SEC of the ED unit was in the range of 0.4–0.6 kWh per m³ and 1,000 ppm of desalted brackish water. Anyway, Fig. 6 shows that a lower V is better to reduce the SEC at any starting brackish solution. On the other hand, Fig. 7 analyzed the duration of the batch tests.

From Fig. 7, it can be seen that tower the applied voltage, higher the duration of desalination test. Similar answer was observed for initial raw water salinity, but it was not maintained as linear as the voltage analysis (a third-order fitting curve was then used). Therefore, the adequate selection of the supplied voltage should be taken depending on the test end objective: lowest SEC, or alternatively maximum drinking water production.

4.3. Influence of the photovoltaic configuration over ED desalination

When the electrolyzer was directly coupled to PV modules, the influence of the feed quality on time and SEC was quite similar than in previous analysis. However, it was not possible to control the applied voltage to the ED stack, since it depended on the I–V curve of the PV generator and the electrical resistance of the solution. The parameters modeling the I–V curve were the environmental conditions (temperature and incident radiation) and the configuration (serial/parallel connection) of the PV generator. As multiple connections could be arranged in that PV array (remember that the number of cells in serial could also be selected), three separated analysis were performed in this section.

First, the number of modules in parallel was studied. Fig. 8 shows the evolution of the dilute concentration and the SEC when a 5,000 ppm solution was desalted up to 250 ppm for two PV configurations: 18

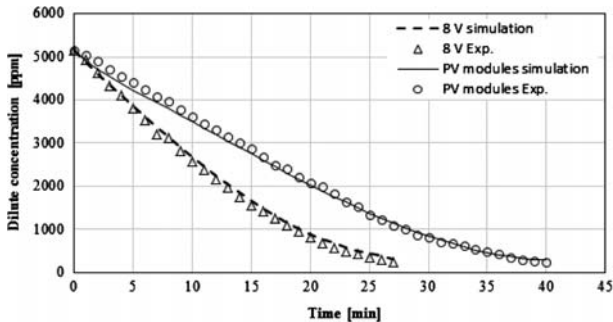


Fig. 5. Theoretical validation of ED stack driven by PV and rectifier models.

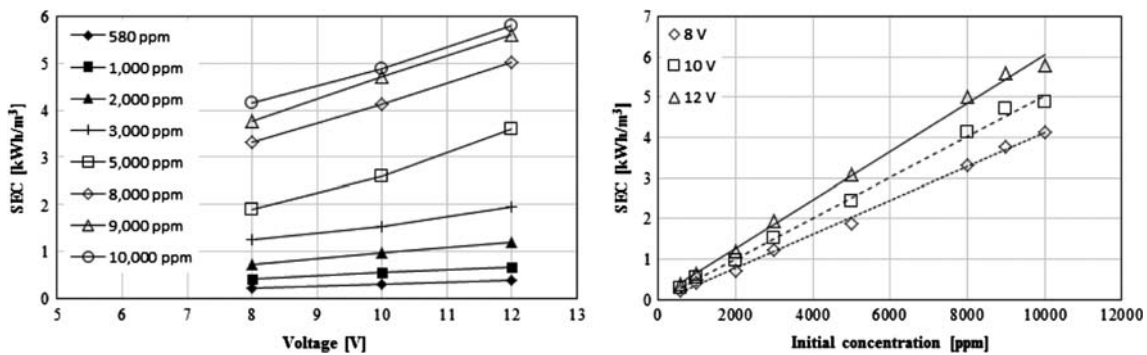


Fig. 6. Voltage (left) and feedwater concentration (right) influence over the SEC.

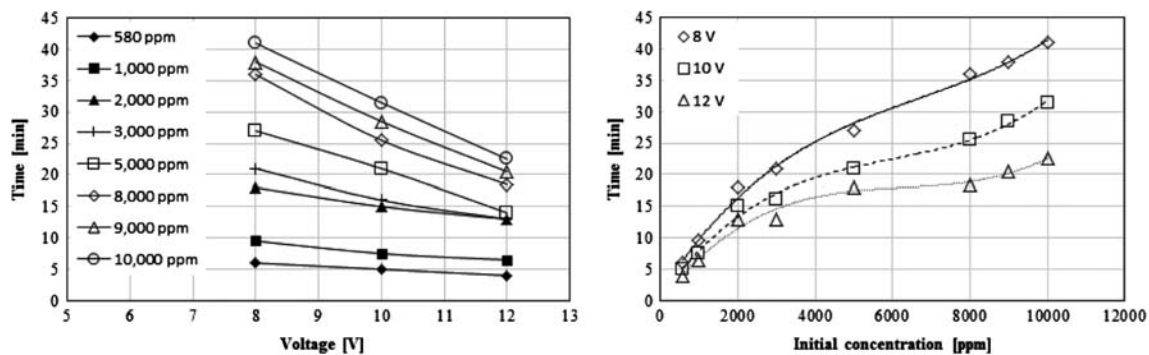


Fig. 7. Voltage (left) and feedwater concentration (right) influence over tests duration.

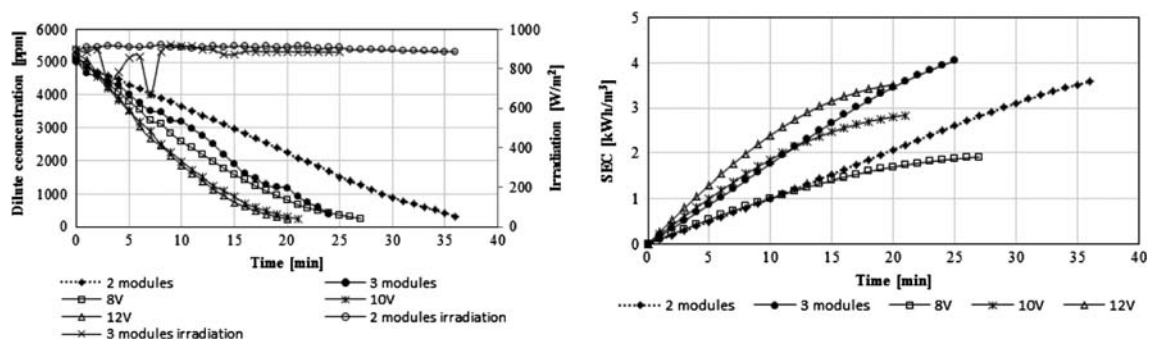


Fig. 8. Power source influence over concentration (left) and SEC (right) batch time.

cells in serial connection, 2 or 3 PV panels. They were also compared with the ED stack fed by the grid at 8, 10, or 12 V, respectively.

As expected, when the number of connected PV modules was increased, the effect over the SEC and batch time reduction was similar to an increase in the applied AC rectified voltage. Table 3 shows the saved CO₂ emissions with respect to the grid connection when the PV array was used in those configurations. An emission factor of 0.223 kg CO₂/kWh_e was taken, according to the Spanish mix [30].

Table 3
Power source test results

Power source	Batch time (min)	SEC (kWh/m ³)	CO ₂ emissions (g CO ₂ /batch)
8 V	27	1.91	0.85
10 V	21	2.84	1.27
12 V	19	3.51	1.57
2 PV modules (20.52 W _p –10.26 V _{oc})	36	3.58	–1.60
3 PV modules (30.78 W _p –10.26 V _{oc})	25	4.05	–1.81

Secondly, the number of cells connected in serial in the PV modules was analyzed. Here, a three PV modules (parallel connection) setup was maintained. Fig. 9 collects the influence of arranging from 18 up to 24 cells in serial over the power provided by the 3 PV modules, in terms of the batch time and the SEC. Tests started at 5,000 ppm and finished at 250 ppm, respectively. Configurations were tested for similar environmental conditions.

As it could be observed, higher PV energy and lower batch time were found if the number of cells increased. Table 4 summarizes the obtained results.

Nevertheless, no large differences were found by using a 18 or a 24 cells configuration in terms of batch time and SEC. Main reason is PV power obtained in the modules decreased as the electrical load increase. This could be perfectly visualized in Fig. 10, where the relation between dilute concentration and electrical resistance (left) and the PV working curve (PV, right) was shown for the previous configurations (number of cells in serial, three parallel connected PV modules) as the water became desalted in the ED batch process. Incoming irradiation and temperature were maintained in order to not overlap three main parameters affecting the performance of a PV array.

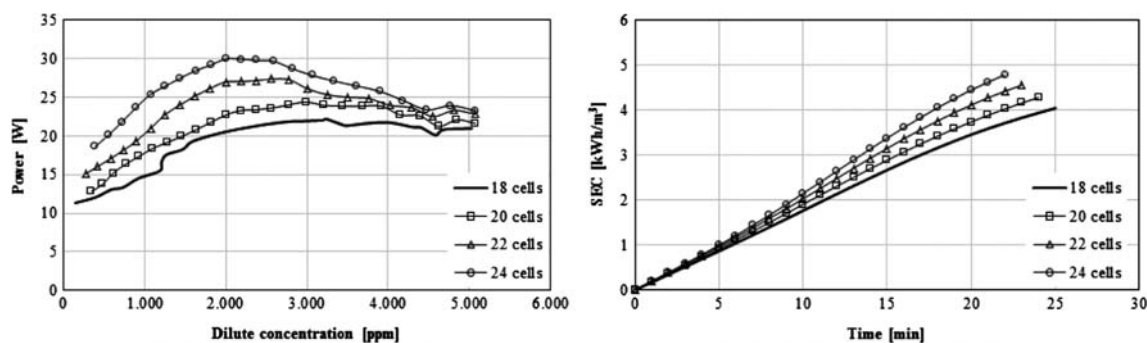


Fig. 9. Number of cells in serial influence over PV power (left), SEC and batch time (right).

Table 4
Number of cells in serial tests results

Number of cells	Batch time (min)	SEC (kWh/m ³)	CO ₂ emissions (g CO ₂ /batch)	Peak power (Pp) (W)	Pp concentration (ppm)
18	25	4.05	−1.81	22.2	3.240
20	24	4.28	−1.90	24.4	2.990
22	23	4.56	−2.03	27.3	2.560
24	22	4.79	−2.14	29.9	2.000

Therefore, and taking into account specific design of the PV modules (multiple connections in serial/parallel), it would be possible to optimize the ED-PV arrangement. That is, depending on the instant dilute concentration, irradiation, and temperature, the optimal PV setup (number of PV modules and the number of cells connected in serial) could be instantaneously connected, in order to obtain the maximum power generation of the PV array, thus using the minimum time per batch (that is, using the highest ED capacity with “free” energy).

In order to clarify that optimum working point of the ED when fed by PV, three PV configurations were taken into consideration: 4×12 , 3×16 , and 2×24 (four modules in parallel with 12 cells in serial, three modules in parallel with 16 cells in serial, and two modules in parallel with 24 cells in serial). These configurations maintained the PV peak power (27.3 Wp) but their characteristic curves (I–V) were obviously different. Fig. 11 (left) shows characteristic I–V curve for each PV configuration and power produced by the PV modules (PV working power is obtained by crossing the characteristic V–I curve with the V/I slope or electrical resistance of the load connected to the PV array). Concentration in the dilute tank were respectively (points in Figure 11, right) 3,500; 3,000; 2,500; 2,000; 1,500; 1,000; 500; and 250 ppm, and the test was performed at low irradiation (around 500 W/m^2).

Therefore, Fig. 11 (right, continuous line) indicates the appropriate configuration along the batch period, in terms of maximum PV generation (e.g. maximum water production). Starting configuration would be 4×12 (low electrical resistance since desalting process was starting, so high current is required to obtain the peak power of the PV array); and the final one would be 2×24 (higher electrical resistance of almost desalted water was found, thus higher voltage was required to obtain the PV power peak).

4.4. Comparison with other ED–PV facilities

Additional tests were performed at diverse PV configurations, as it is shown in Table 6. In the range of a raw water salinity of about 3,000 ppm, SEC were really competitive with respect to the RO alternative: a band from 1 to 1.3 kWh/m^3 was consumed for all configurations. Anyway, the very small size of the pilot plant (batch production is 2 L) forced to compare the results obtained here with higher ED–PV experimental facilities. Analysis was focused on the SEC and batch duration (if possible).

First, the pilot plant was compared with a similar batch ED–PV unit settled at the University of Alicante (Spain). Main differences between both plants are shown in Table 5. Both ED technologies were built by the same manufacturer (Eurodia), and the same ionic

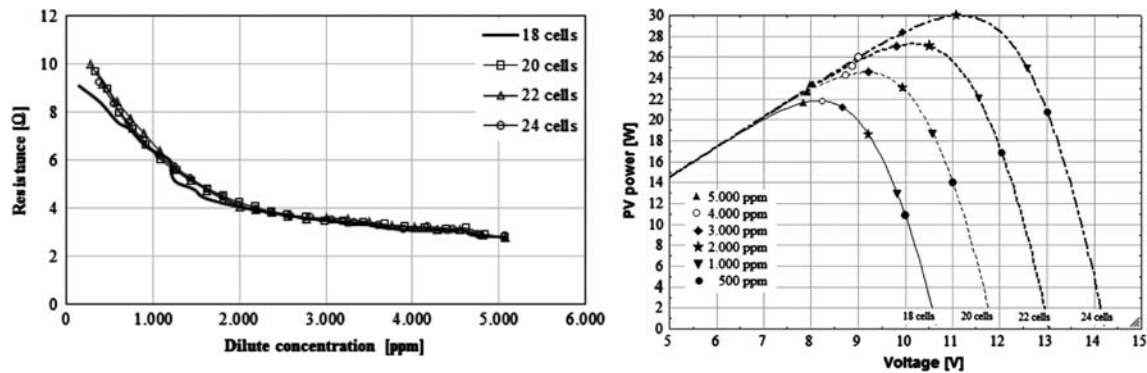


Fig. 10. Number of cells in serial influence over resistance (left) and power of PV modules (right).

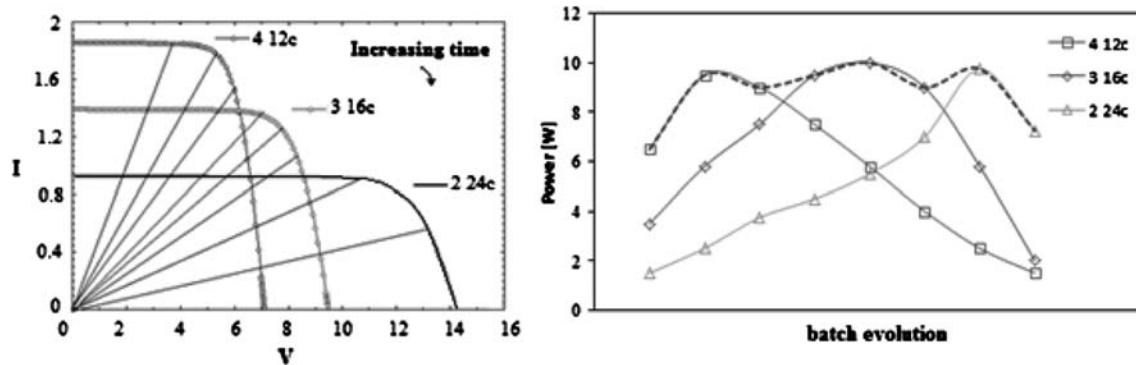


Fig. 11. I–V curves and resistance evolution for each PV configuration (left) and power output evolution (right) along a PV optimized array test.

Table 5
Differences between Circe and University of Alicante pilot plant [9,10,16]

Plant	Batch production (L)	Feeding flow (L/h)	PV coupled (Wp)	Membrane area (m ²)	Membrane pairs
Alicante	150	750	305	3.5	70
Circe-UZ	2	180	40	0.2	10

membranes (Neosepta) were used. It presented a batch production 75 times higher than the Circe's pilot plant, with a dilute feeding flow and a PV system four and seven times higher, respectively.

Their operational parameters were compared in Table 6. End concentration of 400 ppm and a high irradiation (800 W/m²) was found for both plants. The Alicante's pilot plant presented lower SEC values (from 17 to 28%) than the smaller pilot plant (Circe). However, initial concentration for Alicante's plant was approximately 30% lower. Furthermore, batch duration for Circe pilot plant was approximately half (it

varied with the PV configuration) the Alicante's plant batch time. According to those results, it seems that the scale of the batch ED–PV unit is not representative, but the adequate matching between the PV array and the ED stack is compulsory to obtain the best ED performance.

Finally, the batch ED–PV was also compared with a pre-commercial reversal electro dialysis (EDR)–PV pilot plant which was being tested at the Technological Institute of Canarias (ITC) facilities in Pozo Izquierdo (Gran Canaria, Spain). A summary of that plant [31] is shown in Table 7:

Table 6
Operational parameters for Circe and University of Alicante pilot plants

Plant	Feed concentration (ppm)	PV setup	PV power (Wp)	SEC (kWh/m ³)	Batch period (min)
Alicante	2,400	2 × 4	305	0.97	60
Circe	3,072	2 × 24	27.4	1.25	21
Circe	3,180	2 × 20	22.8	1.24	22.5
Circe	3,072	4 × 12	27.4	1.14	36

Table 7
Technical characteristics of the ITC EDR–PV plant

Plant	Feed flow (L/h)	Product flow (L/h)	PV power (Wp)	Membrane pairs
ITC	6,000	4,050	3,700	170

The comparison between both plants was established at similar irradiation (900 W/m²) and end salinity solution (500 ppm). In Table 8 only SEC were compared, since that plant worked as a continuous process in which the feed solution only passed one time across the ED stack. Here, the SEC was around the 60% of the SEC obtained in the batch ED–PV (note that ITC started at lower salinity). Apart from the plant capacity, it is important to remark that the electrical resistance of the EDR unit is almost constant (it was only disturbed by the polarity change of anode and cathode every 15 min), and therefore the matching with the PV array is quite simpler than in the batch ED process.

5. Conclusions

In this paper, a mathematical simulation model was successfully developed to simulate the operation of an ED rectifier and an ED–PV system. The feasibility of the desalination of brackish water by means of a batch ED system powered directly by PV energy was

also successfully tested. Both results (modeling and tests) were in a close agreement. For low brackish waters (1,000–2,000 ppm of salinity), the SEC of a batch ED–PV was really competitive with respect to RO–PV link: around 1 kWh/m³ could be obtained by using free energy, and quite low maintenance for both ED and PV systems was required.

Experimental tests also detected that the batch ED process required the adequate matching of the PV configuration and the ED stack. The maximum PV power should be extracted, which depends of the electrical resistance that has the salty solution at any moment, in order to reduce the batch time, or what is the same, maximize the ED production. The specific design of the PV array in Circe with multiple connections in serial/parallel of the PV cells permitted this kind of analysis.

Finally, it is also important to remark that the use of a small batch ED unit has serious inconveniences (as any batch it is a “manual” plant), but also it is more flexible than a EDR unit, in the sense of the plant does not need to adapt their hydraulic circuit to diverse raw water salinities and/or applied voltages and currents.

Acknowledgments

The authors greatly acknowledge the support given to this work, which is under the framework of the R +D+i project ENE2009-14515-C02-01, financed by the Spanish Ministry of Economy and Competitiveness.

Table 8
Operational parameters for Circe and ITC ED–PV pilot plants

Plant	Feed concentration (ppm)	PV setup	PV power (Wp)	SEC (kWh/m ³)	Batch duration (min)
ITC (EDR–PV)	2,800	N/A	3,700	0.60	N/A
Circe	3,072	2 × 24	27.4	1.25	21
Circe	3,180	2 × 20	22.8	1.24	22.5
Circe	3,072	4 × 12	27.4	1.14	36

Nomenclature

a_m	— active membrane area (m^2)	m	— diode ideality factor
B_0, B_1, B_2	— Falkenhagen equation terms ($\text{\AA}^{-1} \text{mol}^{-1/2}$), ($\text{mol}^{-1/2}$), ($\text{S m}^2 \text{mol}^{-3/2}$)	MD	— membrane distillation
C	— concentration (mol m^{-3})	MED	— multieffect distillation
C_{conc}	— concentration of the concentrate solution at the outlet of the stack (mol m^{-3})	N	— number of cells in ED stack
C_{dil}	— concentration of the dilute solution at the outlet of the stack (mol m^{-3})	q	— electron charge(C)
$C_{\text{conc}}^{\text{AIM}}$	— concentration of the concentrate solution at the anionic membrane surface (mol m^{-3})	$Q_{\text{dil}}, Q_{\text{conc}}$	— dilute and concentrate flow rate ($\text{m}^3 \text{s}^{-1}$)
$C_{\text{dil}}^{\text{AIM}}$	— concentration of the dilute solution at the anionic membrane surface (mol m^{-3})	R_g	— gas-law constant ($\text{mol}^{-1} \text{K}^{-1}$)
$C_{\text{conc}}^{\text{CIM}}$	— concentration of the concentrate solution at the cationic membrane surface (mol m^{-3})	RO	— reverse osmosis
$C_{\text{dil}}^{\text{CIM}}$	— concentration of the dilute solution at the cationic membrane surface (mol m^{-3})	R_c	— electric resistance of the concentrate solution (Ohm)
$C_{\text{conc}}^{\text{in}}$	— concentration of the concentrate solution at the tank (mol m^{-3})	R_{dil}	— electric resistance of the dilute solution (Ohm)
$C_{\text{dil}}^{\text{in}}$	— concentration of the dilute solution at the tank (mol m^{-3})	R_s	— series resistance (Ohm)
CPC	— cylindrical parabolic collector	R_{so}	— seciprocal slope at open-circuit point
D_{a^+}, D_{c^+}	— NaCl anionic and cationic ions diffusion coefficient ($\text{m}^2 \text{s}^{-1}$)	R_{sh}	— photovoltaic module shunt resistance (ohm)
E_D	— Donnan potential (V)	SEC	— specific energy consumption (kWh/m^3)
ED	— electro dialysis process.	T	— temperature (K),
EDR	— reversal ED.	T_c	— PV cell temperature (K)
E_{el}	— cathode and anode reactions potential (V)	$T_{c,\text{ref}}$	— cell temperature at STC conditions (25°C)
E_j	— overall junction potential (V)	t_w	— water transport number
F	— Faraday constant ($96,485 \text{ C mol}^{-1}$)	u	— Falkenhagen equation term (\AA)
G	— irradiation (W/m^2)	V	— voltage (V)
G_{ref}	— STC irradiation ($1,000 \text{ W/m}^2$)	V_{comp}	— volume of space between cells in ED stack (m^3)
H	— distance between ED stack membranes (m)	V_{mp}	— maximum power voltage (V)
h_{a^+}, h_{c^+}	— anionic and cationic membrane thickness (m)	$V_{\text{oc}}, V_{\text{oc,ref}}$	— PV open-circuit cell voltage at any conditions and at STC conditions (V)
I	— current (A)	V_w	— molar volume of pure water ($\text{m}^3 \text{mol}^{-1}$)
I_L	— light-generated current (A)	$V_{\text{conc}}^T, V_{\text{dil}}^T$	— concentrate and dilute volume tank (m^3)
I_{mp}	— maximum power current (A)	V_T	— thermal voltage (V)
I_o	— reverse saturation diode current (A)	z	— ionic charge
$I_{\text{sc}}, I_{\text{sc,ref}}$	— photovoltaic short-circuit current at any conditions and at STC conditions (A)	Greeks symbols	
J_w	— overall water transport through the electromembranes ($\text{mol s}^{-1} \text{m}^{-2}$)	α	— short-circuit current variation coefficient with temperature (A K^{-1})
k	— Boltzmann constant (JK^{-1})	β	— open-circuit voltage variation coefficient with temperature (V K^{-1})
L_w	— membrane constant for water transport by diffusion (m s^{-1})	$A_{\text{dil}}, A_{\text{conc}}$	— molar conductivity of dilute or concentrate solution ($\text{S m}^2 \text{mol}^{-1}$)
		A_o	— molar conductivity at infinite dilution ($\text{S m}^2 \text{mol}^{-1}$)
		$\chi_{\text{conc}}^{\text{AIM}}$	— mean ionic coefficient of the concentrate solution at the anionic membrane surface (S m^{-1})
		$\chi_{\text{dil}}^{\text{AIM}}$	— mean ionic coefficient of the dilute solution at the anionic membrane surface (S m^{-1})

$\lambda_{\text{conc}}^{\text{CIM}}$	— mean ionic coefficient of the concentrate solution at the cationic membrane surface (S m^{-1})
$\lambda_{\text{dil}}^{\text{CIM}}$	— mean ionic coefficient of the dilute solution at the cationic membrane surface (S m^{-1})
$\rho_{\text{AIM}}, \rho_{\text{CIM}}$	— anionic and cationic membrane resistances (Ohm m^2)
ϕ	— current efficiency.

References

- [1] United Nations Development Programme (UNDP), Human Development, Report, 2006.
- [2] D. Alarcón, L. García, J. Blanco, Assessment of an absorption heat pump coupled to a multi-effect distillation unit within AQUASOL project, *Desalination* 212 (2007) 294–302.
- [3] F. Banat, N. Jwaied, M. Rommel, J. Koschikowski, M. Wieg-haus, Desalination by a “compact SMADES” autonomous solar powered membrane distillation unit, *Desalination* 217 (1–3, 5) (2007) 29–37.
- [4] D. Winter, J. Koschikowski, M. Wieg-haus, Desalination using membrane distillation: Experimental studies on full scale spiral wound modules, *Journal of Membrane Science* 375(1–2) (2011) 104–112.
- [5] J. Koschikowski, B. Heijman, Renewable energy drives desalination processes in remote or arid regions, *Membrane Technology* 8 (2008) 8–9.
- [6] G. Kosmadakis, D. Manolakos, G. Papadakis, Parametric theoretical study of a two-stage solar organic Rankine cycle for RO desalination, *Renewable Energy* 35(5) (2010) 989–996.
- [7] D. Manolakos, Sh. Mohamed, I. Karagiannis, G. Papadakis, Technical and economic comparison between PV-RO system and RO-Solar Rankine system. Case study: Thirasia Island, *Desalination* 221(1–3) (2008) 37–46.
- [8] T. Espino, B. Peñate, Optimized desalination of seawater by a PV powered reverse osmosis plant for a decentralized coastal water supply, *Desalination* 156 (2003) 349–350.
- [9] J.M. Ortiz, E. Expósito, F. Gallud, V. García, V. Montiel, A. Aldaz, Electrodialysis of brackish waters powered by photovoltaic energy without batteries: Direct connection behaviour, *Desalination* 208 (2007) 89–100.
- [10] J.M. Ortiz, E. Expósito, F. Gallud, V. García, V. Montiel, A. Aldaz, Desalination of underground brackish water using an electrodialysis system powered directly by photovoltaic energy, *Solar Energy Materials & Solar Cells* 92 (2008) 1677–1688.
- [11] H. Strathmann, *Ion-Exchange Membrane Separation Processes*, Elsevier, Amsterdam, 2004.
- [12] Bayod, A. *Sistemas FV [Photovoltaic (PV) Systems] (in Spanish)*. Prensas Universitarias Eds., University of Zaragoza, 2008.
- [13] Eurodia, *Instruction manual for electrodialysis pilot, Stack EUR2B-10P*, Poitiers, 2010.
- [14] U. Eicker, *Solar Technologies for Buildings*, John Wiley & Sons, London, 2003.
- [15] V. Lo Brano, V. Orioli, G. Ciulla, A. Di Gangi, An improved five parameter model for photovoltaic modules, *Solar Energy Materials and Solar Cells* 94 (2010) 1358–1370.
- [16] M.A. Blas, J.L. Torres, E. Prieto, A. Garcia, Selecting a suitable model for characterizing photovoltaic devices, *Renewable Energy* 25 (2002) 371–380.
- [17] J.M. Ortiz, Desalinización de aguas mediante sistemas de electrodiálisis alimentados directamente con energía solar fotovoltaica: estudio de viabilidad y modelización [Desalination of brackish water by electrodialysis systems directly driven by photovoltaic solar energy: Feasibility study and modeling], M. Sc. Thesis, Instituto Universitario de Electroquímica, Alicante, 2009.
- [18] F.S. Rohman, M.R. Othman, N. Aziz, Modeling of batch electrodialysis for hydrochloric acid recovery, *Chemical Engineering Journal* 162 (2010) 466–479.
- [19] Y. Tanaka, Mass transport and energy consumption in ion-exchange membrane electrodialysis of seawater, *Journal of Membrane Science* 215 (2003) 265–279.
- [20] M. Fidaleo, M. Moresi, Optimal strategy to model the electro-dialytic recovery of a strong electrolyte, *Journal of Membrane Science* 260 (2005) 90–111.
- [21] N. Boniardi, R. Rota, G. Nano, B. Mazza, Lactic acid production by electrodialysis. Part II. Modeling, *Journal of Applied Electrochemistry* 27 (2007) 35–145.
- [22] H.J. Lee, H. Strathmann, S.H. Moon, Determination of the limiting current density in electrodialysis desalination as an empirical function of linear velocity, *Desalination* 190 (2006) 43–50.
- [23] G. Chamoulaud, D. Bélanger, Modification of ion-exchange membrane used for separation of protons and metallic cations and characterization of the membrane by current–voltage curves, *Journal of Colloid and Interface Science* 281 (2005) 179–187.
- [24] V.M. Volgin, A.D. Davydov, Ionic transport through ion-exchange and bipolar membranes, *Journal of Membrane Science* 259 (2005) 110–121.
- [25] G. Kortüm, *Treatise on Electrochemistry*, Elsevier, Amsterdam, 1965.
- [26] J.M. Ortiz, E. Expósito, F. Gallud, V. García, V. Montiel, A. Aldaz, Photovoltaic electrodialysis system for brackish water desalination: Modeling of global process, *Journal of Membrane Science* 274 (2008) 138–149.
- [27] A.W. Adamson, *Química Física [A Textbook of Physical Chemistry]* Vol. 1, Reverté, España, 1979.
- [28] G. Kortüm, *Treatise on Electrochemistry*, Elsevier, Amsterdam, 1965.
- [29] PVSYST, Study of photovoltaic systems, Software package, Ver. 5.4, Switzerland: University of Geneva; 2011.
- [30] WWF-Adena, Observatory of electricity. Annual report. 2011, Spain.
- [31] J. Veza, B. Peñate, F. Castellano, Electrodialysis desalination designed for off-grid wind energy, *Desalination* 160 (2004) 211–221.